KSCE Journal of Civil Engineering (2020) 24(3):807-815
DOI 10.1007/s12205-020-1797-0

pISSN 1226-7988, eISSN 1976-3808
www.springer.com/12205

Geotechnical Engineering

Micro-Level Analysis of Marine Clay Stabilised with Polyurethane

Samaila Saleh[a,b], Nor Zurairahetty Mohd Yunus[a], Kamarudin Ahmad[a], Nazri Ali[a], and Aminaton Marto[c]

[a]*Dept. of Geotechnics and Transportation, Universiti Teknologi Malaysia, Johor Bahru 81310, Malaysia*
[b]*Dept. of Civil Engineering, Hassan Usman Katsina Polytechnic, Katsina 820241, Nigeria*
[c]*Malaysia-Japan International Institute of Technology, Universiti Teknologi Malaysia, Kuala Lumpur 54100, Malaysia*

ARTICLE HISTORY

Received 8 October 2019
Revised 1 December 2019
Accepted 7 January 2020
Published Online 14 February 2020

KEYWORDS

Marine clay
Polyurethane
Unconfined compressive strength
X-ray diffraction analysis
Field emission scanning electron microscopy
Energy dispersive spectroscopy

ABSTRACT

Soil stabilisation is one type of ground improvement technique regarded as effective in minimising foundation problems associated with marine clay (MC). In this paper, in-depth micro-level analysis was conducted on MC stabilised with 8% Polyurethane (PU). The effectiveness of PU as a stabiliser was evaluated using unconfined compressive strength (UCS) tests and one-dimensional consolidation tests. Mineralogy of MC was studied using X-ray diffraction analysis (XRD). Furthermore, field emission scanning electron microscopy (FESEM) and energy dispersive spectroscopy (EDX) were used to discern the roots of improvement in the strength of MC. The result of XRD analysis identified the presence of Quartz, Montmorillonite, Calcite and Clinochlore. FESEM results discovered that MC showed crumpled, curled and flaked soil particles that have a fuzzy arrangement and cusp-like crystals in a joined fashion. The contact among the particles is surface-to-surface and surface-to-edge. The PU foam was composed of intramolecular closed cells that are non-homogeneous, non-identical, and of inconsistent average diameters of about 2.3 μm. Finally, EDX results revealed that O, C, Si, Al, Fe and N are the elements that contributed more than 96% of the composition of MC and PU.

1. Introduction

The problem of marine clay (MC) is well-known worldwide. Occurrence of MC causes severe destruction to lightly-loaded structures, comparable to natural disasters like flood or earthquakes (Gunturi et al., 2015). MC is a type of expansive soil present in coastal areas that is characterised by poor engineering properties like high settlement, and meagre shear strength (Wu et al., 2015a; Guo and Wu, 2017; Guo and Wu, 2018; Jamaludin et al., 2019). Constructing any infrastructure with MC is an extremely challenging task due to the effect of moisture variation on the swelling and shrinkage characteristics of the soil. MC expands or contracts when the moisture content increases or decreases due to seasonal variation (Mohammed Al-Bared and Marto, 2017; Saleh et al., 2019b). Due to the unsuitability of using MC in its natural state, in many instances, MC is improved with the aid of admixtures or aggregates, or by mechanical means, making it possible to use for construction purposes.

Numerous studies have been conducted on stabilised MC using various admixtures such as lime (Yi et al., 2015), cement (Zhou et al., 2019), sodium silicate (Pakir et al., 2015), and bio-encapsulation (Ivanov et al., 2015) among others. However, the high cost and long curing time of most chemical stabilisers have forced researchers to continue investigations into the problem of MC. Nevertheless, the auspicious qualities of PU, like high strength and short hardening time, are attracting the attention of many researchers. For example, injecting PU was used in soft soil to stabilise tunnel excavation (Li et al., 2016; Bayati and Khademi Hamidi, 2017). Injecting PU also reinforced a slope, retaining wall, jointed rock and sandy soil (Chun et al., 1997; Kazemian et al., 2010). PU micropile improved the bearing capacity and reduced the settlement of silty clayey soil (Valentino and Stevanoni, 2016), PU grout repaired road pavements (Vennapusa et al., 2016; Mohamed Jais, 2017) and airport pavements (Priddy et al., 2010). PU also enhanced MC shear strength by more than 200% (Saleh et al., 2018). Still, there is limited information about the fundamentals of how stabilisation with PU is achieved.

The research context shown above has led to further interest in investigating the morphology and changes in the microstructure

CORRESPONDENCE Samaila Saleh samailasaleh@graduate.utm.my Dept. of Geotechnics and Transportation, Universiti Teknologi Malaysia, Johor Bahru 81310, Malaysia; Dept. of Civil Engineering, Hassan Usman Katsina Polytechnic, Katsina 820241, Nigeria

of MC stabilised with PU. This paper proposes a micro-level study of MC stabilised with PU. In this research, XRD, FESEM and EDX were carried out to explore the morphology and changes associated with MC stabilised with PU.

2. Materials and Method

The following section describes the materials used in the research and methods to prepare them.

2.1 Materials

The materials used for this study were MC and PU. The MC sample, collected from Batu Pahat, Johor Bahru, Malaysia, was air-dried, pulverised mechanically, sieved over a 2 mm sieve, and then stored in an airtight plastic container. PU comprised two components: Polyol and Isocyanate. Properties of MC and PU were reported by Saleh et al. (2018, 2019a) and are presented in Table 1.

Table 1. Materials Properties

Properties	Unit	Value	Reference
Liquid limit	%	65	(Saleh et al., 2018)
Plastic limit	%	26	
Fine fraction	%	98.68	
OMC	%	25	
MDD	Kg/m^3	1440	
Viscosity of polyol	mPas	260 ± 50	
Polyol specific gravity	-	1.15	
Viscosity of Isocyanate	mPas	185 ± 35	
Isocyanate specific gravity	-	1.24	
pH	-	3.25	(Saleh et al., 2019a)
Loss on ignition	%	8	
Sulphate ions	mg/l	6,071	
Chloride ion	mg/l	287	
Nitrate ions.	mg/l	22	
Marine clay classification	-	CH	

2.2 Method

Dry MC was mixed with optimum moisture content (OMC) water and placed in an airtight plastic container for 24 hours for permeation, under controlled conditions of 20°C and more than 90% humidity according to the American Society for Testing and Materials (ASTM, 2017). Wet MC was then mixed with a varying dosage of PU compacted in a cylindrical mould with a height of 76 mm and diameter of 38 mm. Fig. 1 shows various stages of the sample preparation for the UCS test. The specimens were cured for one, three and seven days and then tested using the UCS test. Untreated MC was tested immediately after demoulding. The loading of the test was conducted under strain control at a rate of 1.52 mm/min.

The consolidation test was performed based on British standard procedures (BS1377-5, 1990). Unsaturated samples were used for the consolidation test, using a method of sample preparation adopted

Fig. 1. Sample Preparation for the UCS Test: (a) Pulverised Marine Clay, (b) Moist Marine Clay, (c) PU Foam Added to MC, (d) Mixing PU Foam and MC, (e) Compacting MC-PU Mixture using Hydraulic Jack, (f) Extruding the Compacted MC-PU Mixture from Mould

by Estabragh et al. (2020); Olgun and Yıldız (2010). Specimens for the consolidation test were prepared by pre-consolidating them in a cylindrical mould using static compaction and transferred to rings of 50 mm in diameter and 20 mm in height. The mould had removable collars at both ends and the same diameter as the oedometer ring. PU (8%) was added to MC and mixed with the treated specimen before being compacted in the mould.

The specimens tested with the UCS test were dried and used for FESEM and EDX analysis. Mineralogical composition of the MC was identified with the aid of a diffraction pattern. A beam of XRD (Cu K_α radiation) was passed through the sample; the detector was scanned through an angle 2 theta ranging between 10 and 90 degrees at a rate of 8 degrees per minute. Individually crystals have a distinctive pattern of diffraction angles and an equivalent concentration of the diffracted beam (intensity). In that manner, mineralogy of MC was analysed as per the standard Powder Diffraction File (JCPDS, 1995). The plot was drawn by taking the position of 2 theta angles along the abscissa and intensity in terms of counts along the ordinate. XRD gave different peaks for the different basal spacing.

The FESEM machine examines the morphological nature of MC. The embedded EDX in the FESEM machine enabled the characterisation of elemental compositions of MC.

3. Results and Discussions

The analysis and discussion of results of MC treated with PU are presented in this section.

3.1 Influence of Polyurethane on Shear Strength of Marine Clay

Preliminary assessment of strength improvement was conducted through the UCS test. Fig. 2 displays the UCS result of the treatment of MC with a different dose of PU cured for one, three and seven days. The result shows that an increase in the dose of PU caused an improvement in the shear strength of MC. Conversely, an increase in the dose of PU also caused a corresponding decrease in the axial strain of MC. For example, during the 3-day curing period, an increase in PU content from 4% to 12% caused an improvement in strength of MC from 125 kPa to 216 kPa.

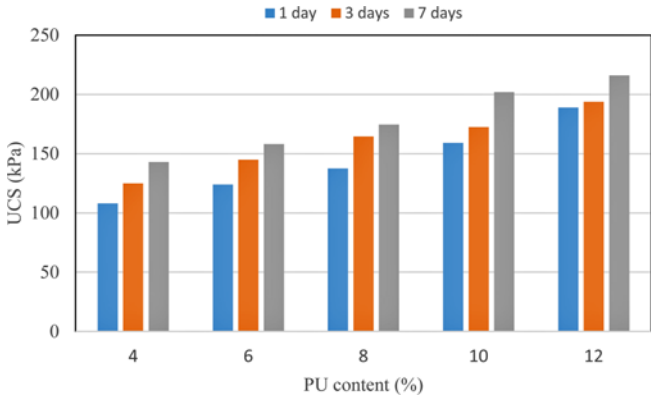

Fig. 2. Effect of PU on the Unconfined Compressive Strength of MC

Continuous increase in PU content causes improvement in strength, and decrease in axial strain of MC. However, when PU content extended beyond 8%, the mixture of soil and PU started forcing itself out of the mould due to increase in the volume of the mixture of MC and PU, as shown in Fig. 3(a). Consequently, the mould could not accommodate the mixture of PU and MC. Increase in the volume of the MC-PU mixture is due to normal characteristics of PU, which increased in volume by about 20 times from its original size (Vipulanandan et al., 2012; Babcock,

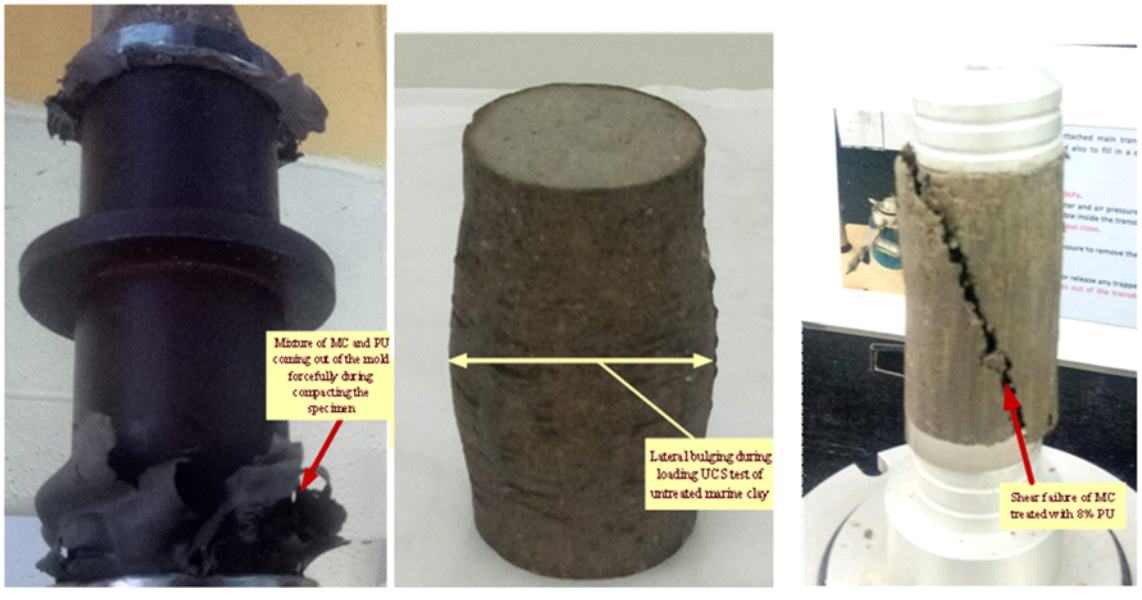

Fig. 3. Behavior of Marine Clay during Treatment with PU: (a) Mixture of MC and PU Coming Out of the Mold, (b) Bulging Failure of Untreated Marine Clay, (c) Shear Failure of MC Untreated with PU

2018). Therefore 8% PU content was adopted for further tests during this research.

The result also shows that increase in curing time leads to a corresponding improvement in strength of MC. For example, using 8% PU increased MC UCS from 66 kPa to 137.5 kPa, 165 kPa and 174 kPa during the one, three and seven days curing periods, respectively. Moreover, the treatment of MC with PU also changed the failure pattern of MC from bulging to shear failure. Untreated MC underwent lengthy axial deformation, accompanied by lateral bulging, as shown in Fig. 3(b). Meanwhile, PU-treated MC created higher deviator stress and little axial deformation that came with shear failure, as shown in Fig. 3(c).

3.2 Effect of Polyurethane on Consolidation Characteristics of Marine Clay

Figure 4 shows the results of the one-dimensional consolidation test of both untreated MC and MC treated with 8% PU. The results show that consolidation curves of MC treated with 8% PU are located above untreated MC. This is similar to the behaviour of expansive clay soil treated with acetone (Estabragh et al., 2020). Compression and swelling indexes (C_c and C_r) of untreated MC are 0.2682 and 0.0049, respectively, while compression and swelling indexes (C_c and C_r) of MC treated with 8% PU are 0.0061 and 0.0017, respectively. The trend of the results is also similar to that reported by Estabragh et al. (2020) on the effect of organic chemical on mechanical properties of expansive clay.

3.3 Mineralogy of Marine Clay Using X-Ray Diffraction Analysis

Figure 5 displays the results of MC XRD patterns. Significant peaks were observed at values of 2 thetas, shown in Table 2. The peaks were indexed using a $\sin^2\theta$ method (Ramesh and Punithamurthy, 2017; Kundu et al., 2018), and the result is shown in Table 2. Among all peaks, the peak at 2 theta, equal to 26.54° was the highest, followed by that at 20.8°. The 2 sharp narrow peaks at 2 theta, equal to 20.8° and 26.54°, are characteristic peaks of Quartz (SiO_2) (Nian et al., 2019). Remarkably, diffraction peaks indicating quartz were very sharp, signifying its excellent crystalline structure (Yang et al., 2017). Other reasonably high peaks from XRD results are at 36.50°, 39.42°, 42.41°, 54.87° and 59.93°.

Unique diffraction angles (2 theta) and indexing pattern (Table 2) were used to study the mineralogy of MC as per the standard Powder Diffraction File (JCPDS, 1995). For example, existence of peaks at 19.8° and 34.9° established the presence of Montmorillonite, $(Na, Ca)0,3(Al, Mg)_2Si_4O_{10}(OH)_2{\cdot}n(H_2O)$ mineral group in MC (Rahman et al., 2013; Mohd Yunus et al., 2015;

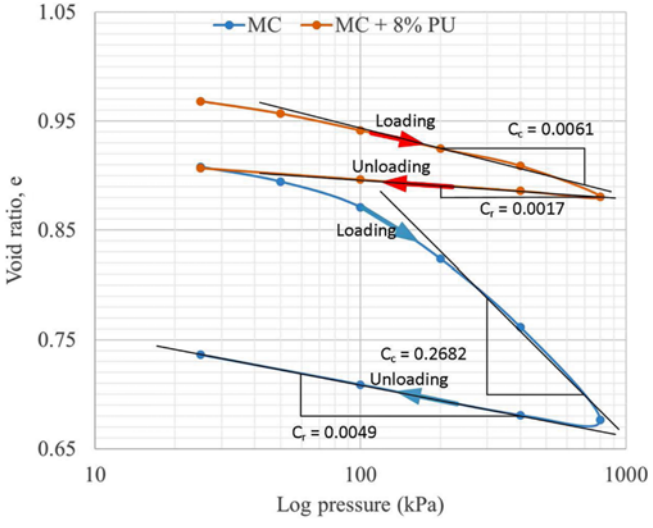

Fig. 4. Results of the One Dimensional Consolidation Test

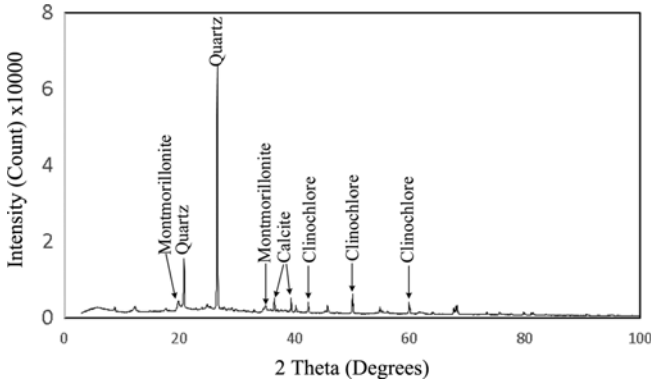

Fig. 5. XRD Result of MC

Table 2. Indexing the MC XRD Result

2Theta (deg.)	Theta (rad.)	$\sin^2\theta$	Ratio 1	Ratio 2	Ratio 3	m	hkl
19.80	0.17279	0.0296	1.00	2.00	3.00	1	100
20.80	0.18148	0.0326	1.10	2.20	3.31	1	100
26.59	0.23203	0.0529	1.79	3.58	5.37	2	110
34.93	0.30482	0.0901	3.05	6.09	9.14	3	111
36.50	0.31850	0.0981	3.32	6.63	9.95	3	111
39.42	0.34404	0.1138	3.85	7.70	11.55	4	200
42.41	0.37008	0.1308	4.43	8.85	13.28	4	200
50.10	0.43719	0.1793	6.06	12.13	18.19	6	211
59.93	0.52298	0.2495	8.44	16.88	25.32	8	220

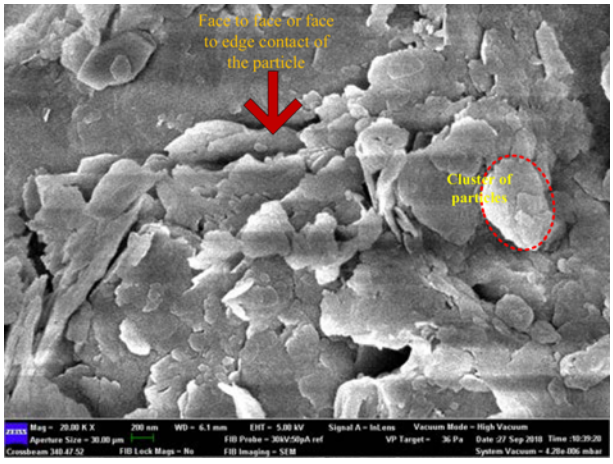

Fig. 6. FESEM Image of the Untreated MC

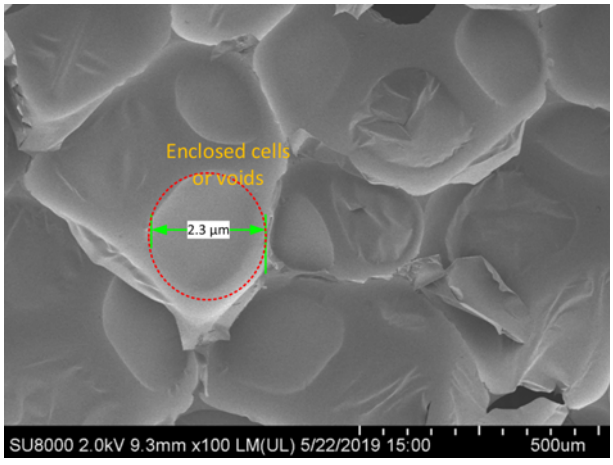

Fig. 7. FESEM Image of PU

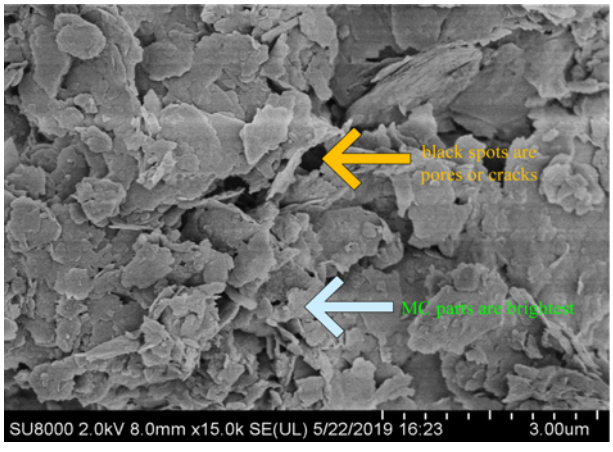

Fig. 8. FESEM Image of the MC Treated with 8% PU

Murmu et al., 2019). Similarly, Calcite ($CaCO_3$) was present for peaks at 2 theta equal to 36.5°, and 39.42° (Cai and Liu, 2017; Nian et al., 2019) and Clinochlore, (Mg, Fe^{2+})$5Al_2Si_3O_{10}(OH)_8$ for peaks at 42.1°, 50.1° and 59.93° (Nian et al., 2019).

Furthermore, using Eq. (1), the crystallinity of MC was computed as 30.16%

$$Crystallinity = \frac{A_p}{A_t} \times 100\% \quad (1)$$

A_p is the area of crystalline peaks, equal to 20,703.05 nm^2 and A_t is the total area of all peaks, equal to 68,649.48 nm^2. Values for the areas were computed using a peak analysis with origin Pro software. Therefore, the crystallinity of MC was computed at 30.16%.

3.4 Field Emission Scanning Electron Microscopy Analysis

The microstructure of MC was observed using the FESEM analysis. Fig. 6 shows the results of FESEM analysis for untreated MC. Based on the results, the fundamental unit of MC showed uneven, curled and flaked units. Particle clusters had negatively charged surfaces and were arranged to form a structure of honeycomb pores (Nian et al., 2019). Individual particles of the soil had a fuzzy arrangement and cusp-like crystals in a joined fashion. The bunches consisted of small pieces, similar to units with distinct edges, as shown in Fig. 6. The connections among the units were primarily surface-to-surface and surface-to-edge, and the contact of the particles determines the flocculated structure (Lei et al., 2018).

Figure 7 displays FESEM results of PU. From the PU image, it is clear that PU was composed of closed cells or voids. The voids were small, non-identical, distributed, and with an inconsistent diameter of about 2.3 µm. The presence of moderately rough and non-homogeneous intramolecular voids are typical characteristics of ductile material like PU (Wu et al., 2015b). The voids are mostly polygon- or spherical-shaped, with large contact surface areas. Statistical analysis of foam cells using image J software based on the method of Wei et al. (2017) showed that average minimum and maximum sizes of the voids were 1.5 µm and 3.4 µm, respectively. The shape of PU images is similar to that observed by other researchers (Vlad et al., 2011; He et al., 2016; Wei et al., 2017).

Figure 8 shows the FESEM image of treated MC. The image illumination can identify the components of the images. MC parts appear brightest, while the black spots show as pores or cracks (Cai and Liu, 2017). A comparison of the images of untreated and treated MC is given in Figs. 6 and 8. The 2 images show no significant difference, only a re-arrangement of individual particles. This means there is no evidence of the formation of a new compound due to the reaction between MC and PU. However, the image of untreated MC is brighter than that of treated MC. Coating MC particles with PU foam, while mixing the dual could be the reason that makes the treated sample slightly darker. Again, proportional areas of the pores and cracks (black sports part of the images) computed using image J software were 3.6% and 6.6% for treated and untreated MC, respectively, as presented in Table 3 and Fig. 9. Smaller percentages of the areas of the pores in treated MC confirm that microstructure of the treated MC is denser than untreated MC. This is in agreement with findings by Shaikh et al. (2014).

Table 3. Computation of Pores and Cracks (black sports part of the images)

Sample	Count	Total Area (μm^2)	Average Size (μm^2)	%Area (%)	Mean (μm)	Perimeter (μm)	Circularity
Untreated MC	4210	2.627	6.24E-04	6.604	254.191	0.069	0.887
Treated MC	1615	1.823	0.001	3.613	254.259	0.096	0.847

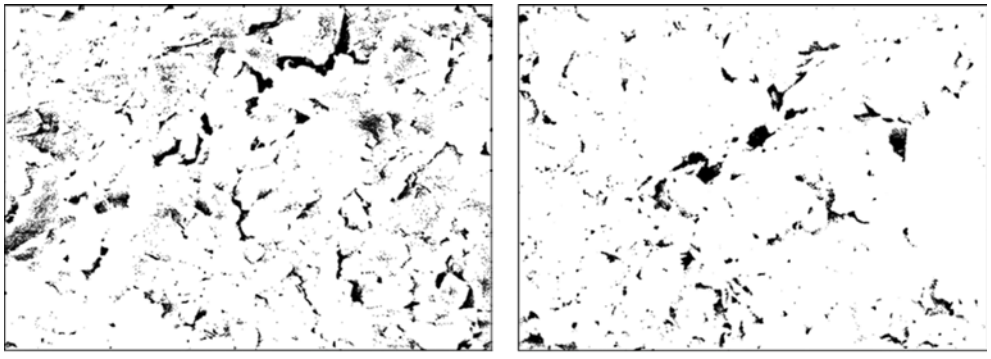

(a) (b)

Fig. 9. Black Sports Part of the Images: (a) Untreated MC, (b) Treated MC

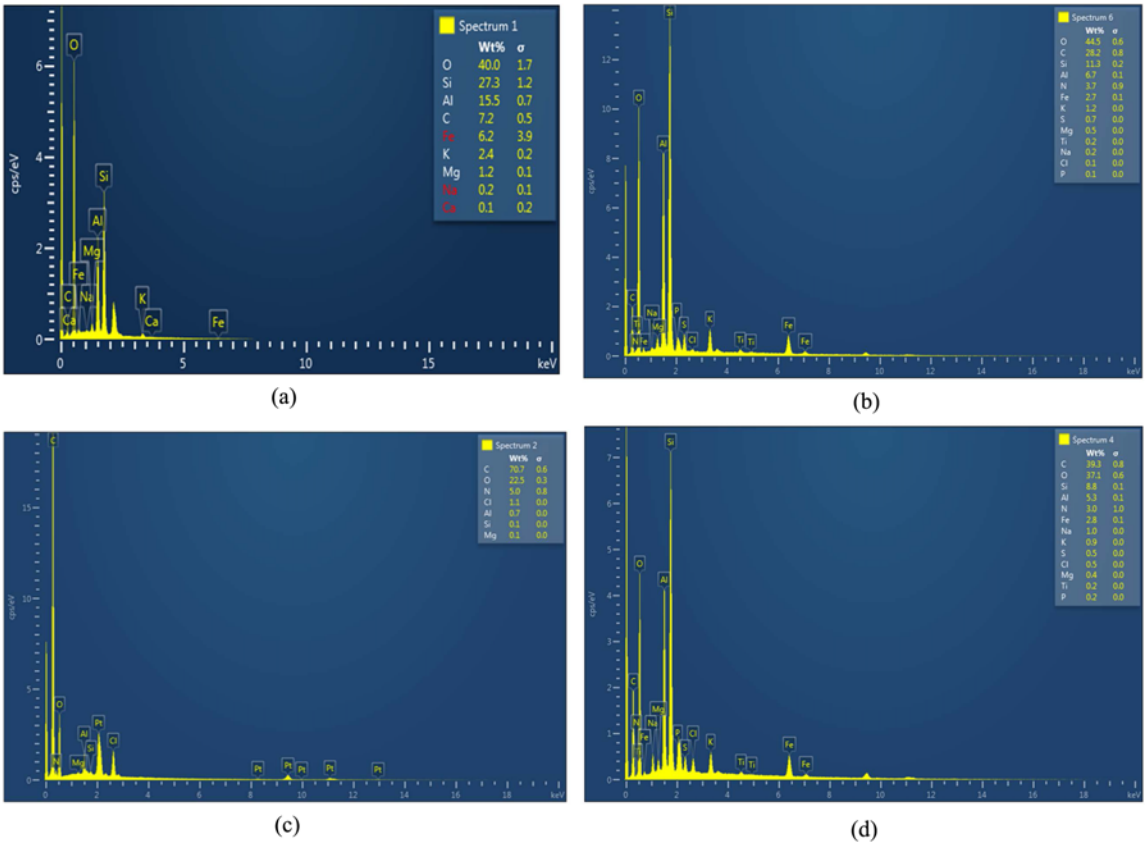

(a) (b)

(c) (d)

Fig. 10. EDX Result for: (a) Untreated MC, (b) Treated MC, (c) PU at the Edge of the Enclosed Cells, (d) PU at the Center of Enclosed Cells (voids) (a) EDX of Untreated MC, (b) EDX of MC Treated with 8% PU, (c) EDX of PU at the Edge of the Enclosed Cells, (d) PU at the Centre of Enclosed Cells (voids)

The cluster size of MC particles is relatively bigger before treatment with PU. After the treatment of MC with the 8% PU, there is a decrease and narrowing in the size and distribution of MC-PU composite particles. The reduction in the size of MC-PU composite particles caused a rise in the densification of treated MC, and consequent enhancement of the shear strength of MC treated with PU (He et al., 2016).

3.5 Energy Dispersive Spectroscopy Analysis

EDX is a microanalysis method used in combination with FESEM. EDX analysis identifies x-rays released from the specimen through electron beam bombing to characterise the composition of elements in the sample (MEEI, 2014). Figs. 10(a) and 10(d) display EDX results of MC (before and after treatment) and PU. It can be seen that the total quantity of significant elements (O, C, Si Al and Fe) contributed to 96.2% within the MC specimens. The elemental nature of MC is similar to that reported by Phetchuay et al. (2016).

On the other hand, the elemental composition of PU was captured around the centre of the enclosed cells or pores and at the edge of the pores. The elemental composition of PU at the centre of the enclosed cells or void is different from that at the edge of the enclosed cells. The elemental composition of PU at the edge of the enclosed cells showed O, C, N and Cl contributed 22.5%, 70.7%, 5% and 1.1%, respectively. The result is comparable to that of other studies (He et al., 2016). In contrast, the elemental composition of PU at the centre of the enclosed cells showed that O, C, Si, Al, Fe and N contributed 39.3%, 37.1%, 8.8%, 5.3%, 2.8% and 3%, respectively. The distribution of all elements present in each sample of MC and PU is shown in Fig. 10.

Results of EDX analysis (see Fig. 11) show that after oxygen, core components of both untreated and treated MC are Si, Al, and Fe. There is an apparent decrease in concentration levels of Si, Al and Fe before and after the treatment of MC with PU. Concentration of the elements changes from 27.3% to 11.3%, 15.5% to 6.7% and 6.2% to 2.7% for Si, Al, and Fe, respectively.

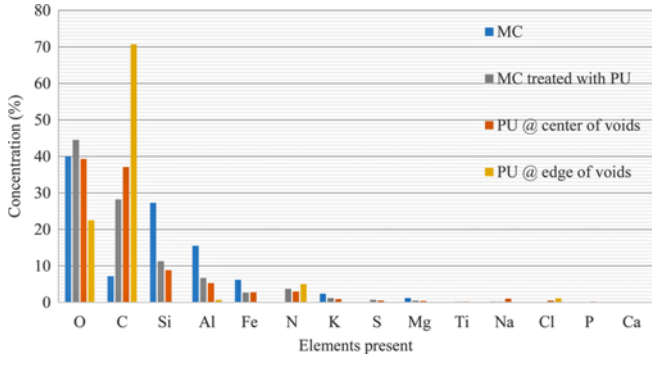

Fig. 11. EDX Results of the PU, Untreated and Treated MC

Table 4. Core Components of MC before and after Treatment with PU

ELEMENTS	Untreated MC	MC treated with PU
O	40	44.5
C	7.2	28.2
Si	27.3	11.3
Al	15.5	6.7
Fe	6.2	2.7
N	0	3.7
Si/Al ratio	1.8	1.7
Si/Fe ratio	4.4	4.2

Moreover, there is also an apparent increase in the concentration of C and N from 7.2% to 28.2%, and 0% to 3.7% for untreated and treated MC, respectively. However, ratios of Si/Al and Si/Fe for both untreated and treated MC remain similar, as presented in Table 4. Retaining the same ratios of Si/Al and Si/Fe before and after the treatment of MC with PU is another verification that Si, Al and Fe ions did not dissolve during the treatment of MC with PU (Ahmari and Zhang, 2013; Zhang et al., 2018). Si, Al and Fe ions are core cementation ions required for a pozzollanic reaction (Hemalatha and Santhanam, 2018; Bensaifi et al., 2019). Therefore, if ratios of Si/Al and Si/Fe remain unchanged before and after the treatment of MC with PU, it indicates that treatment of MC with PU did not result in a pozzollanic reaction. Non-occurrence of pozzollanic reaction during the treatment of MC with PU is also established, as there was no aqueous environment of pH 12.4 – a requisite for cementation reaction to take place (Ling et al., 2014).

4. Conclusions

Results of a micro-level analysis of MC stabilised with 8% PU are presented in this paper. From the research findings, the following conclusions are made:

1. The UCS results revealed an improvement in shear strength of MC from 66 kPa to 145 kPa, 164.5 kPa, 172.5 kPa and 193.7 kPa during the three-day curing period, due to the addition of 6%, 8%, 10% and 12% PU, respectively. Additionally, 8% PU improved the shear strength of MC from 66 kPa to 137.5 kPa, 165kPa and 174 kPa during the one, three and seven days curing periods.
2. The results of the one-dimensional consolidation test revealed that treatment of MC with 8% PU reduces compression indexes from 0.2682 to 0.0061, and swelling indexes from 0.0049 to 0.0017, respectively.
3. The result of XRD identified the presence of quartz (SiO_2) as the significant crystalline material in MC for peaks at 2 thetas equal to 20.8° and 26.54°. Other minerals detected in MC were Montmorillonite, $(Na, Ca)0,3(Al, Mg)_2Si_4O_{10}(OH)_2{\cdot}n(H_2O)$ for 2 theta peaks equal to 19.8° and 34.93°, Calcite ($CaCO_3$) for peaks at 2 theta equal to 36.5°, and 39.42° and Clinochlore, $(Mg, Fe^{2+})5Al_2Si_3O_{10}(OH)_8$ for peaks at 2 theta equal to 42.1°, 50.1° and 59.93°. Moreover, the crystallinity of MC is 30.16%
4. The FESEM results revealed that MC showed crumpled, curled and flaked soil particles with a fuzzy arrangement and cusp-like crystals in a joined fashion. The contact among the particles is surface-to-surface and surface-to-edge. The PU foam is composed of intramolecular closed cells or voids that are nonhomogeneous, non-identical, distributed, and of inconsistent diameters of about 2.3 μm on average. Treatment of MC with PU did not cause the formation of a new compound, but it caused re-arrangement and increase in the densification of the soil particles, resulting in improvement in shear strength.

5. EDX results revealed that O, C, Si, Al and Fe are elements that contributed more than 96% of the elemental composition of MC, while O, C, N and Cl contributed 98.8% of the elemental composition of PU. There was also an apparent decrease in the concentration of Si, Fe and Al ions, and increase in the concentration of C and N after treatment of MC with PU. However, the ratios of Si/Al and Si/Fe for both untreated and treated MC remain alike, indicating that Si Al and Fe ions did not dissolve during the treatment of MC with PU.

Acknowledgements

The authors are grateful to the funding of Fundamental Research Grant Universiti Teknologi Malaysia Malaysia, Vot no R.J130000.7851.5F197. The first author is also grateful to the support of Tertiary education trust fund (TFUND) Nigeria.

Nomenclature

ASTM = American Society for Testing and Materials
C_c = Compression index
C_r = Swelling index
EDX = Energy Dispersive Spectroscopy
FESEM = Field Emission Scanning Electron Microscopy
JCPDS = Joint Committee on Powder Diffraction Standards
MC = Marine Clay
MDD = Maximum Dry Density
OMC = Optimum Moisture Content
PU = Polyurethane
UCS = Unconfined Compressive Strength
XRD = X-Ray Diffraction analysis

ORCID

Not Applicable

References

Ahmari S, Zhang L (2013) Utilization of cement kiln dust (CKD) to enhance mine tailings-based geopolymer bricks. *Construction and Building Materials* 40:1002-1011, DOI: 10.1016/j.conbuildmat.2012.11.069

ASTM (2017) Standard practice for making and curing soil-cement compression and flexure test specimens in the laboratory. D1632-17, American Society for Testing and Materials, West Conshohocken, PA, USA

Babcock BN (2018) Cement grout vs chemical grout: Which one to use, when, and why. In: A white paper providing guidance to the geotechnical community, Avanti International, Houston, TX, USA

Bayati M, Khademi Hamidi J (2017) A case study on TBM tunnelling in fault zones and lessons learned from ground improvement. *Tunnelling and Underground Space Technology* 63:162-170, DOI: 10.1016/j.tust.2016.12.006

Bensaifi E, Bouteldja F, Nouaouria MS, Breul P (2019) Influence of crushed granulated blast furnace slag and calcined eggshell waste on mechanical properties of a compacted marl. *Transportation Geotechnics* 20:100244, DOI: 10.1016/j.trgeo.2019.100244

BS1377-5 (1990) Compressibility, permeability and durability tests. BS1377-5, British Standard Institution, London, UK

Cai G, Liu S (2017) Compaction and mechanical characteristics and stabilization mechanism of carbonated reactive MgO-stabilized silt. *KSCE Journal of Civil Engineering* 21(11):2641-2654, DOI: 10.1007/s12205-017-1145-1

Chun B, Ryu DS, Shin C, Im G, Choi J, Lim H (1997) The performance of polyurethane injection method with soil nailing system for ground reinforcement. *Ground Improvement Geosystems*, 445-451

Estabragh AR, Afsari E, Javadi AA, Babalar M (2020) Effect of Two organic chemical fluids on the mechanical properties of an expansive clay soil. *Journal of Testing and Evaluation* 48(5):20170623, DOI: 10.1520/JTE20170623

Guo L, Wu DQ (2017) Study of recycling Singapore solid waste as land reclamation filling material. *Sustainable Environment Research* 27(1):1-6, DOI: 10.1016/j.serj.2016.10.003

Guo L, Wu DQ (2018) Study of leaching scenarios for the application of incineration bottom ash and marine clay for land reclamation. *Sustainable Environment Research* 28(6):396-402, DOI: 10.1016/j.serj.2018.06.004

Gunturi M, Ravichandran PT, K DK, Annadurai R, Rajkumar PRK (2015) Micro level analysis of RBI 81 stabilized expansive soil. *International Journal of ChemTech Research* 7(2):666-672

He Z, Li Q, Wang J, Yin N, Jiang S, Kang M (2016) Effect of silane treatment on the mechanical properties of polyurethane/water glass grouting materials. *Construction and Building Materials* 116:110-120, DOI: 10.1016/j.conbuildmat.2016.04.112

Hemalatha MS, Santhanam M (2018) Characterizing supplementary cementing materials in blended mortars. *Construction and Building Materials* 191:440-459, DOI: 10.1016/j.conbuildmat.2018.09.208

Ivanov V, Chu J, Stabnikov V, Li B (2015) Strengthening of soft marine clay using bioencapsulation. *Marine Georesources & Geotechnology* 33(4):320-324, DOI: 10.1080/1064119X.2013.877107

Jamaludin N, Mohd Yunus NZ, Jusoh SN, Pakir F, Ayub A, Zainuddin NE, Hezmi MA, Mashros N (2019) Potential and future: Utilization of waste material on strength characteristics of marine clay. *IOP Conference Series: Materials Science and Engineering* 527:012003, DOI: 10.1088/1757-899X/527/1/012003

JCPDS (1995) Standard X-ray diffraction powder patterns. International centre for diffraction data, US Department of Commerce, Washington, DC, USA

Kazemian S, Huat BBK, Prasad A, Barghchi M (2010) A review of stabilization of soft soils by injection of chemical grouting. *Australian Journal of Basic and Applied Sciences* 6(12):5862-5868

Kundu SP, Chakraborty S, Chakraborty S (2018) Effectiveness of the surface modified jute fibre as fibre reinforcement in controlling the physical and mechanical properties of concrete paver blocks. *Construction and Building Materials* 191:554-563, DOI: 10.1016/j.conbuildmat.2018.10.045

Lei H, Feng S, Jiang Y (2018) Geotechnical characteristics and consolidation properties of Tianjin marine clay. *Geomechanics and Engineering* 16(2):125-140, DOI: 10.12989/gae.2018.16.2.125

Li S, Liu R, Zhang Q, Zhang X (2016) Protection against water or mud inrush in tunnels by grouting: A review. *Journal of Rock Mechanics and Geotechnical Engineering* 8(5):753-766, DOI: 10.1016/j.jrmge.2016.05.002

Ling FNL, Kassim KA, Karim ATA, Ho SC (2014) Evaluation of

contributing factors on strength development of lime stabilized artificial organic soils using statistical design of experiment approach. *Advanced Materials Research* 905:362-368, DOI: 10.4028/www.scientific.net/AMR.905.362

MEEI (2014) Energy dispersive x-ray spectroscopy - handbook of analytical methods for materials. Materials Evaluation and Engineering, Inc., Plymouth, MN, USA, 17-18

Mohd Yunus NZ, Marto A, Pakir F, Kasran K, Jamal MAA, Jusoh SN, Abdullah N (2015) Performance of lime-treated marine clay on strength and compressibility chracteristics. *International Journal of Geomate* 8(2):1232-1238, DOI: 10.21660/2015.16.4132

Mohamed Jais IB (2017) Rapid remediation using polyurethane foam/resin grout in Malaysia. *Geotechnical Research* 4(2):107-117, DOI: 10.1680/jgere.17.00003

Mohammed Al-Bared MA, Marto A (2017) A review on the geotechnical and engineering characteristics of marine clay and the modern methods of improvements. *Malaysian Journal of Fundamental and Applied Sciences* 13(4):825-831, DOI: 10.11113/mjfas.v13n4.921

Murmu AL, Jain A, Patel A (2019) Mechanical properties of alkali activated fly ash geopolymer stabilized expansive clay. *KSCE Journal of Civil Engineering* 23(9):3875-3888, DOI: 10.1007/s12205-019-2251-z

Nian T, Jiao H, Fan N, Guo X (2019) Microstructure analysis on the dynamic behavior of marine clay in the South China Sea. *Marine Georesources & Geotechnology,* 1-14, DOI: 10.1080/1064119X.2019.1573864

Olgun M, Yıldız M (2010) Effect of organic fluids on the geotechnical behavior of a highly plastic clayey soil. *Applied Clay Science* 48(4):615-621, DOI: 10.1016/j.clay.2010.03.015

Pakir F, Marto A, Mohd Yunus NZ, Tajudin SAA, Tan CS (2015) Effect of sodium silicate as liquid based stabilizer on shear strength of marine clay. *Jurnal Teknologi* 76(2):45-50

Phetchuay C, Horpibulsuk S, Arulrajah A, Suksiripattanapong C, Udomchai A (2016) Strength development in soft marine clay stabilized by fly ash and calcium carbide residue based geopolymer. *Applied Clay* 127(128):134-142, DOI: 10.1016/j.clay.2016.04.005

Priddy LP, Jersey SR, Reese CM (2010) Full-scale field testing for injected foam stabilization of portland cement concrete repairs. *Transportation Research Record: Journal of the Transportation Research Board* 2155(1):24-33, DOI: 10.3141/2155-03

Ramesh S, Punithamurthy K (2017) The effect of organoclay on thermal and mechanical behaviours of thermoplastic polyurethane nanocomposites. *Digest Journal of Nanomaterials and Biostructures* 12(2):331-338

Rahman ZA, Yaacob WZW, Rahim SA, Lihan T, Idris WMR, Mohd Sani WNF (2013) Geotechnical characterisation of marine clay as potential liner material. *Sains Malaysiana* 42(8):1081-1089

Saleh S, Asmawisham Alel MN, Mohd Yunus NZ, Ahmad K, Ali N, Abang Hasbollah DZ, Asnida Abdullah R (2019a) Geochemistry characterisation of marine clay. *IOP Conference Series: Materials Science and Engineering* 527:012023, DOI: 10.1088/1757-899X/527/1/012023

Saleh S, Mohd Yunus NZ, Ahmad K, Ali N (2018) Stabilization of marine clay soil using polyurethane. *MATEC Web of Conferences* 250:01004, DOI: 10.1051/matecconf/201825001004

Saleh S, Mohd Yunus NZ, Ahmad K, Ali N (2019b) Improving the strength of weak soil using polyurethane grouts: A review. *Construction and Building Materials* 202:738-752, DOI: 10.1016/j.conbuildmat.2019.01.048

Shaikh FUA, Supit SWM, Sarker PK (2014) A study on the effect of nano silica on compressive strength of high volume fly ash mortars and concretes. *Materials & Design* 60:433-442, DOI: 10.1016/j.matdes.2014.04.025

Valentino R, Stevanoni D (2016) Behaviour of reinforced polyurethane resin micropiles. *Proceedings of the Institution of Civil Engineers - Geotechnical Engineering* 169(2):187-200, DOI: 10.1680/jgeen.14.00185

Vennapusa PKR, Zhang Y, White DJ (2016) Comparison of pavement slab stabilization using cementitious grout and injected polyurethane foam. *Journal of Performance of Constructed Facilities* 30(6):04016056, DOI: 10.1061/(ASCE)CF.1943-5509.0000916

Vipulanandan C, Kazez MB, Henning S (2012) Pressure-temperature-volume change relationship for a hydrophilic polyurethane grout. Proceedings of the 4th international conference on grouting and deep mixing, February 15-18, Reston, VA, USA, 1808-1818

Vlad S, Ciobanu C, Butnaru M, Macocinschi D, Filip D, Gradinaru LM, Mandru M (2011) Preparation of polyurethane microspheres by electrospray technique. *Digest Journal of Nanomaterials and Biostructures* 6(2):643-652

Wei Y, Wang F, Gao X, Zhong Y (2017) Microstructure and fatigue performance of polyurethane grout materials under compression. *Journal of Materials in Civil Engineering* 29(9):04017101, DOI: 10.1061/(ASCE)MT.1943-5533.0001954

Wu D, Xu W, Tjuar R (2015a) Improvements of marine clay slurries using chemical–physical combined method (CPCM). *Journal of Rock Mechanics and Geotechnical Engineering* 7(2):220-225, DOI: 10.1016/j.jrmge.2015.02.001

Wu H, Zhu M, Liu Z, Yin J (2015b) Developing a polymer-based crack repairing material using interpenetrate polymer network (IPN) technology. *Construction and Building Materials* 84:192-200, DOI: 10.1016/j.conbuildmat.2015.03.067

Yang Z, Zhang X, Liu X, Guan X, Zhang C, Niu Y (2017) Flexible and stretchable polyurethane/waterglass grouting material. *Construction and Building Materials* 138:240-246, DOI: 10.1016/j.conbuildmat.2017.01.113

Yi Y, Gu L, Liu S (2015) Microstructural and mechanical properties of marine soft clay stabilized by lime-activated ground granulated blastfurnace slag. *Applied Clay Science* 103:71-76, DOI: 10.1016/j.clay.2014.11.005

Zhang M, Zhao M, Zhang G, Sietins JM, Granados-Focil S, Pepi MS, Xu Y, Tao M (2018) Reaction kinetics of red mud-fly ash based geopolymers: Effects of curing temperature on chemical bonding, porosity, and mechanical strength. *Cement and Concrete Composites* 93:175-185, DOI: 10.1016/j.cemconcomp.2018.07.008

Zhou N, Ouyang S, Cheng Q, Ju F (2019) Experimental study on mechanical behavior of a new backfilling material: Cement-treated marine clay. *Advances in Materials Science and Engineering* 2019:1-8, DOI: 10.1155/2019/1261694